Applied Catalysis B: Environmental 160–161 (2014) 730–741

Contents lists available at ScienceDirect

Applied Catalysis B: Environmental

journal homepage: www.elsevier.com/locate/apcatb

Review

Recent advances in silver-based heterogeneous catalysts for green chemistry processes

Chao Wen, Anyuan Yin, Wei-Lin Dai*

Department of Chemistry and Shanghai Key Laboratory of Molecular Catalysis and Innovative Materials, Fudan University, Shanghai 200433, PR China

ARTICLE INFO

Article history:
Received 31 March 2014
Received in revised form 11 June 2014
Accepted 14 June 2014
Available online 20 June 2014

Keywords:
Silver catalyst
Chemo-selective oxidation
Hydrogenation
Photo-catalysis
Electro-catalysis

ABSTRACT

Silver-based heterogeneous catalysts play an important role in the catalytic elimination of environmental pollutants, production of clean energy, fuel distillation and the synthesis of highly value chemical intermediates. Most silver catalysts are mainly applied in the following four domains: chemo-selective oxidation, hydrogenation, photo-catalysis and electro-catalysis. The development of Ag-based heterogeneous catalysts would definitely contribute to the environment improvement and efficient utilization of energy resources. It would also help balance environment concerns with economic development. This mini-review gives an overview of recent progress in silver-based heterogeneous catalysts for four green chemical processes.

Contents

1. Introduction

With increasing importance being placed on energy and environmental issues, more and more green chemical processes are urgently needed to meet the challenging green requirements, especially in the catalysis industry. So-called green chemistry approaches have significant potential not only for the reduction of byproducts and energy consumption, but also for the development of new methodologies toward previously unobtainable materials using existing technologies. Green chemistry promotes environmental and economic prosperity coupled with sustainable chemical methodologies. Catalysis is one of the key underpinning technologies on which new approaches to green chemistry are based. Recently, significant progress has been made in several key fields including green catalysis, the design of safer chemicals and environmentally benign solvents, and the development of renewable feedstocks such as biomass. In all, it is necessary to design catalysts and catalysis processes with environmental considerations in mind.

Redox processes such as selective hydrogenation and oxidation are two of the key synthetic steps for the activation of a broad range of substrates. They are used for the production of either final products or intermediates. Molecular hydrogen and oxygen are good industrial options for hydrogenolysis and oxidation, respectively

* Corresponding author. Tel.: +86 5566 4678; fax: +86 5566 5572.
E-mail address: wldai@fudan.edu.cn (W.-L. Dai).

http://dx.doi.org/10.1016/j.apcatb.2014.06.016
0926-3373/

because of their high atomic economy. However, H_2 has to be activated on the surface of a heterogeneous catalyst prior to reaction under typical conditions. The O_2 however, is a di-radical in its groundstate and can participate in radical processes readily, even under very mild reaction conditions. However, the industrial application of the Ag based heterogeneous catalysts is scarce which is mainly confined to the epoxidation of ethylene, methanol oxidation to formaldehyde or other oxidation reactions [1]. Furthermore, Ag based catalysts, which own the catalytic reduction properties, also exhibit superb catalytic performances in the field of hydrogenation process, photocatalytic reaction and electro-catalysis. In this review, the interaction between silver and H_2/O_2 is given to better understand the silver-based heterogeneous catalysis.

Silver is a group IB transition metal with a $4d^{10}5s^1$ electronic layer structure. Silver-based materials with different morphology (nanobar, nanocubic, nanosphere etc.) have been a popular functional materials applied in many fields especially for heterogeneous catalysis due to its specific physical and chemical structure. However, compared with a research on gold nanoparticle catalysis, less attempts [1–12] have been focused on the catalysis of silver clusters or nanoparticles and structure–performance relationship of these catalysts. The performance of silver catalysts depends strongly on their surface structure and surface sites, which are very sensitive to the preparation method, pretreatment or reaction conditions, and the size of silver nanoparticles. Compared with other metals, such as nickel, palladium and platinum, silver is lack of affinity toward H_2 due to the filled d-band. Theoretical calculation [13–15] shows that the hydrogen interacts only very weakly with extended silver surfaces (single crystals, polycrystalline surfaces), and no dissociative chemisorption could occur at low temperature, which was attributed to the completely filled d-band of silver as well as the position of the d-band center relative to the Fermi level. However, pretreatment of silver in O_2 atmosphere would affect the interaction of silver with hydrogen. In other words, the activation of silver catalysts is often regarded as a result of the presence of various Ag-O interactions, for example, the molecular surface and subsurface oxygen atoms, etc. [16,17] In addition, due to its surface plasmon resonance (SPR) (When a noble metallic-nanoparticle is excited by light, the oscillating electric field of the light interacts with the conduction electrons.), a strong oscillation of these electrons happens when the incident photon frequency is resonant with the collective oscillation of the conduction electrons. Such resonance is called localized surface plasmon resonance. For metallic nanoparticles, the silver nanoparticles have also been applied widely in the field of photocatalysis.

In this review, a selection of the most recent advances in the field of silver-based heterogeneous catalysts for green chemistry process gives experimentalists a proper guide and overview to silver catalysis.

2. Environmental catalysis

2.1. Green oxidation catalysis

Silver-based materials are an outstanding catalyst for many catalytic oxidation reactions, such as ethylene epoxidation [18], formaldehyde synthesis [19], NO_x abatement [20], the selective catalytic oxidation of ammonia [21], partial oxidation of benzyl alcohol [22], the oxidative coupling of methane [23], the oxidation of styrene [24], the selective oxidation of ethylene glycol [25] and CO oxidation [26–30]. The surface and subsurface oxygen atoms found by Ertl and Schlögl were investigated to be the active sites for Ag catalysts in many oxidation reactions [31–34], and different pre-treatment atmosphere and temperatures affect the formation of subsurface oxygen and activated silver catalysts. It is understood that oxygen pre-treatment at high temperature results in the formation of subsurface oxygen that then activates silver catalysts [35,36]. The role of different silver species has also been studied, and Ag^0 as an active species was found to enhance the catalytic activity at low temperature (<140 °C). In contrast, Ag^+ could be the active species at temperatures about 140 °C on Ag/Al_2O_3 for the selective oxidation of ammonia to nitrogen [21]. The conversion of NO to N_2 was enhanced on the reduced silver species resulting from thermal-induced changes in silver morphology for NO_x abatement [20].

The catalytic oxidation of CO to CO_2 at low temperature is an important subject for environmental protection. It has widespread applications in air purification for buildings or vehicles and in reformer gas for fuel cell plants [26–30]. The Ag/TiO_2 catalysts have shown 50% CO conversion at 60 °C. Higher activities for CO oxidation at 100 °C over Ag/Mn/perovskite have also been obtained. Even 90% CO conversion at 126 °C could be obtained via Ag/α-MnO_2 [26]. Recently, Au-Ag alloy catalysts prepared by a unique deposition-precipitation method or the post-graft method showed better catalytic activity for CO oxidation at room temperature [27–29]. Liu et al. [30] reported that highly dispersed silver catalysts with mesostructured silica supports by a one pot synthesis approach exhibited 100% CO conversion at room temperature. Zhang et al. [37] studied the influence of pretreatment conditions on the catalytic performance of CO oxidation over Ag/SiO_2 and concluded that oxygen-containing Ag species might be the active species and silver particle size ca. 4.5–5.5 nm would be favorable for the low temperature CO oxidation. In addition, Hu et al. [38] developed the Ag/OSM-2 catalyst with a cryptomelane type structure via a reflux approach for the selective oxidation of CO in the hydrogen rich steam. In long term stability testing under realistic reaction conditions, 100% CO conversion can be maintained for 250 h at 120 °C with 90% selectivity.

Formaldehyde is an important chemical intermediate and is extensively used for the synthesis of value-added chemicals such as ethylene glycol, glycolic acid, dyes, and drugs. The synthesis of anhydrous formaldehyde via the direct dehydrogenation of methanol is a promising approach, and the development of highly efficient catalysts is of great importance. Silver-based catalysts seem to be a good choice for the direct dehydrogenation of methanol [39–42]. The $Ag\text{-}SiO_2\text{-}Al_2O_3$ material prepared by our group seems to be a powerful catalyst for the selective oxidation of methanol with excellent stability in methanol oxidation and no appreciable deactivation or structural changes even after reaction for more than 140 h [19]. It is noted that methanol adsorption on the surface of pure silver is insignificant but is facilitated by the presence of small amounts of oxygen in the reaction mixture. It is commonly accepted that there are various oxygen species formed on the silver surface after the adsorption of oxygen [43,44] such as weakly bound atomic species (O^α), bulk dissolved species (O^β) and strongly bound species (O^γ). Oxygen—usually termed the subsurface oxygen species—is the most stable species at high reaction temperatures and dehydrogenates methanol to anhydrous formaldehyde.

Many types of silver catalysts are used in the process of direct dehydrogenation of methanol to anhydrous formaldehyde. A catalyst made of silver gauze with an additional, electrolytically deposited silver layer [45] shows 84% formaldehyde yield at 800 °C and an elevated pressure in the gas–vapor mixture. Similar results can also be obtained (78%) when the dehydrogenation of steam-diluted methanol is performed at 620 °C in the presence of silver on copper gauze [43]. In addition, eutectic Ag_3Cu_2 alloy granules (0.8–2.4 mm) were also tested as a catalyst in the dehydrogenation of nitrogen diluted methanol [44]. However, sintering of the alloy is observed when a high formaldehyde yield (60%) is attained. A more stable $Ag_{97}Cu_2Si$ catalyst giving a 58% formaldehyde yield

can be obtained when admixed with silicon after increasing the silver content in the catalyst [44]. More recently, several supported Ag catalysts have been applied to the direct dehydrogenation of methanol. The $AgMg_{25}Si_4O_{10}F_2$ sample was synthesized by ion exchange in an aqueous $AgNO_3$ solution. Upon utilization at 550 °C it showed high selectivity for formaldehyde although the methanol conversion did not exceed 5% [46]. It is assumed that Ag^+ cations introduced into the mica in the preparation stage undergo reduction during the catalytic process. Then the highly dispersed particles of metallic silver appear, on which the direct dehydrogenation of methanol takes place. A Ag-SiO_2-ZnO catalyst prepared by an impregnation method shows a 39% yield of formaldehyde and 48% conversion of methanol at 600 °C [47].

Our group reported a novel Ag/SiO_2-MgO with 96% conversion of methanol and 78% selectivity for formaldehyde at 650 °C [39]. Differing from Sago et al. [47], the Ag/SiO_2-ZnO catalyst prepared by the sol–gel method shows a rather high activity with 82% conversion of methanol and 89% selectivity to formaldehyde. It is interesting that the catalytic performance changes with the ratio of the components in the ternary system (Ag/SiO_2-M_xO_y). For instance, an Ag/SiO_2-Al_2O_3 catalyst shows 95% conversion of methanol and 81% yield of formaldehyde. Dimethyl ether (DME) is the main by-product on the catalyst due to the presence of typical acidic centers on Al_2O_3 [40]. Once zinc is added to the Ag/SiO_2-Al_2O_3 catalyst, the Ag-SiO_2-Al_2O_3-ZnO catalyst presents higher activity with 99% conversion of methanol and 87% selectivity toward formaldehyde [41]. The basic centers on zinc oxide neutralize part of the acidic centers of Al_2O_3 and then restrict the generation of the byproduct as DME.

Our group also developed an efficient Ag-SiO_2-MgO-Al_2O_3 catalyst by tuning the relative ratio of the components [42]. The catalyst with a mass ratio of Ag:SiO_2:MgO:Al_2O_3 = 20:55.2:8.3:16.5 shows 100% methanol conversion and 100% selectivity to formaldehyde. The composition of the Ag-SiO_2-MgO-Al_2O_3 catalyst is crucial for the catalytic performance. The optimal content of MgO was determined to be 15 wt.% of the SiO_2 content, and the optimal Al_2O_3 content was 30 wt.% of SiO_2. Lower or higher contents of Al_2O_3 both decreased the selectivity for formaldehyde.

For some catalytic applications, bimetallic alloy nanoparticles of Ag with a second metal component have been extensively investigated to improve their catalytic performance. These systems form new active sites, improve the electronic structure and have important synergistic effects. Among these bimetallic nanocatalysts, AgAu alloys show catalytic performance for oxygen transfer reaction superior to that of their monometallic counterparts. The degree of enhancement is strongly correlated with the surface silver content [48–56]. In addition, the synthetic approach of monodispersed Ag-containing alloy nanoparticles with controlled particle size and composition is still of key issue in the study of catalytic mechanisms and the kinetics of reaction. Liotta et al. [57] reported a pumice-supported PdAg alloy applied to the selective oxidation of benzyl alcohol to benzaldehyde. The introduction of Ag into the Pd/Pumice catalyst offered a beneficial effect that was attributed to a modified electron density. Recently, colloidal Au-Ag nanoparticles stabilized with poly(N-vinyl-2-pyrrolidone)(PVP) in an aqueous solution have been reported as catalysts for the oxidation of benzyl alcohol with molecular oxygen. However, the PVP-stabilized Au-Ag alloy nanoparticles offered catalytic activity only in the presence of a strong base (KOH or K_2CO_3) [58]. Huang et al. [59] reported a facile method for synthesizing highly stable monodispersed Au-Ag alloy nanoparticles of varied Ag/Au molar ratios with a high total metal concentration of 5×10^{-4} M. The as-prepared Au-Ag nanoparticles have comparable particle sizes of 3–4 nm and show activity for benzyl alcohol oxidation as a model reaction with molecular oxygen in the absence of base. The presence of Ag (Ag/Au molar ratio ≤ 10:90) significantly enhances the catalytic activity of the Au-Ag

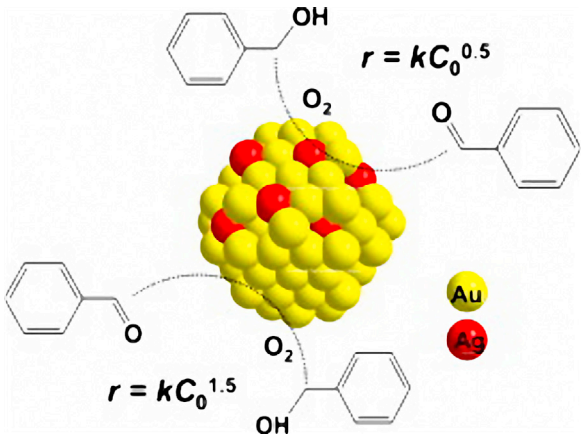

Fig. 1. Proposed aerobic oxidation kinetics of benzyl alcohol on the surface of Au and Au/Ag alloy nanoparticles [59].

nanoparticles. X-ray photoelectron spectroscopy (XPS) analysis reveals that Au atoms transfer electrons toward neighboring Ag atoms resulting in a different reaction mechanism and different kinetics for aerobic oxidation of benzyl alcohol from those of pure Au nanocatalyst. The oxidation of benzyl alcohol follows 1.5-order reaction kinetics on the active sites using Au alone, while on Au active sites adjacent to Ag atoms a 0.5-order reaction is observed with respect to benzyl alcohol. The proposed aerobic oxidation kinetics of benzyl alcohol on the surface of AuAg alloy nanoparticles are shown in Fig. 1.

Hirasawa et al. [60] reported an efficient Pd-Ag alloy catalyst applied to the selective oxidation of glycerol to dihydroxyacetone (DHA) under neutral conditions. The physical mixture of Pd/C and Ag/C showed almost no enhancing effect on the DHA selectivity and activity and clearly demonstrated this vital function in the synergetic effects of Pd-Ag alloy in the synthesis of DHA from glycerol. The synergetic reaction mechanism of the aerobic glycerol oxidation over Pd-Ag/C is the dehydrogenation mechanism wherein both substrate and oxygen are activated on the catalyst surface. The terminal OH group of glycerol is adsorbed on Ag, and the 2-position of the adsorbed glycerol reacts with dissociatively adsorbed oxygen over Pd atoms. The proposed mechanism of glycerol oxidation over Pd-Ag/C catalyst is shown in Fig. 2.

Recently, many researchers have reported that Ag catalysts show good activity for soot oxidation at lower temperatures. Aneggi et al. [61] studied the effect of Ag addition on the soot oxidation activity over various metal oxides. The addition of Ag to ZrO_2 and Al_2O_3 resulted in very active catalysts, while the addition to CeO_2 had little benefit. On the other hand, Machida et al. [62] and Shimizu et al. [63] reported that CeO_2-supported Ag catalyst enhanced the catalytic activity for soot oxidation. Considering silver sintering under high temperature, Yamazaki et al. [64] developed CeO_2-Ag catalyst with a Ag core and CeO_2 shell morphology via a novel nanofabrication method. This product had exceptional performance for soot oxidation with gaseous oxygen at temperatures below 300 °C in tight and loose contact modes. This morphology was designed to increase the Ag/CeO_2 interface area per unit surface area of Ag particles and inhibited Ag sintering due to the stable CeO_2 particles as barriers. A possible mechanism for soot oxidation was proposed (see Fig. 3), where the active oxygen species formed on the Ag surface from gaseous O_2 migrated to the CeO_2 surface via the interface transformation into O_n^{x-} species. This then further migrated onto soot particles where the oxidation occurred. The abundantly formed O_n^{x-} species quickly migrate out to the external surface and efficiently access soot particles. The surface migration process is a key factor in its excellent soot oxidation performance and compactness between catalyst and soot.

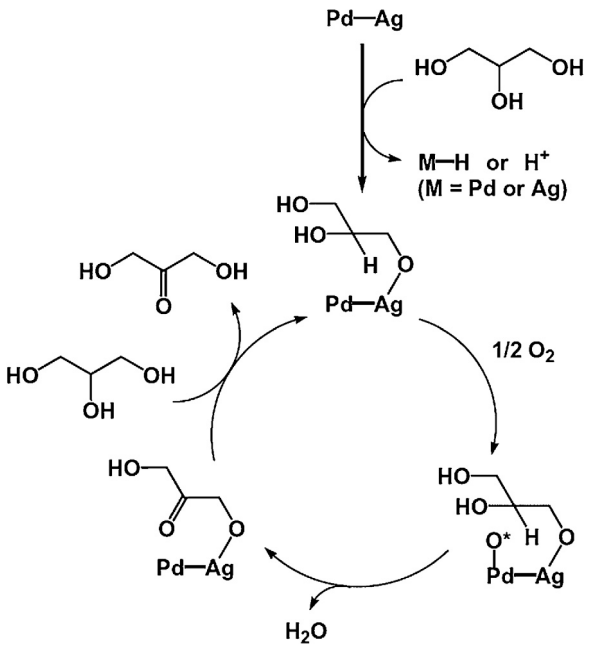

Fig. 2. Proposed mechanism of glycerol oxidation over Pd-Ag/C [60].

2.2. Green hydrogenation catalysis

Silver has drawn less attention as a catalyst for hydrogenation than the platinum group metal catalysts. However, the Clause group first reported the excellent selectivity of silver nanoparticle catalysts for the hydrogenation of C=O group in the presence of a C=C bond [3]. For the selective hydrogenation of crotonaldehyde by 1–7 nm TiO_2- or SiO_2-supported silver particles, the larger particle size gave higher selectivity to the desired product—unsaturated alcohol [3]. However, the relationship between the Ag particle size and the catalytic activity is quite complicated. Chen et al. reported that 7–9 nm silver nanoparticles on Ag/SiO_2 catalyzed the selective hydrogenation of chloro-nitrobenzenes to their corresponding chloroanilines and they believed that the size of the silver nanoparticles as well as the interaction between the silver nanoparticles and the catalyst support may play an important role in the catalytic reaction system [6].

Selective hydrogenation of the nitro group via H_2 in the presence of other reducible functional groups is an important reaction to produce functionalized anilines as industrial intermediates for a variety of specific and fine chemicals [65]. Shimizu et al. [66] systematically investigated size- and support-dependent silver cluster catalysts for chemoselective hydrogenation of nitroaromatics. They found that silver clusters supported on θ-Al_2O_3 exhibited highly chemoselective reductive activity on the nitro group for the reduction of substituted nitroaromatics. Cooperation of the acid-base pair sites on Al_2O_3 and the coordinatively unsaturated Ag sites on the silver cluster is responsible for the rate-limiting H_2 dissociation to yield a H^+/H^- pair at the metal/support interface, while the basic site on Al_2O_3 acts as an adsorption site of nitroaromatics. These fundamental aspects are very close to those for Al_2O_3-supported gold nanoparticle catalyst [67]. This finding provides a strategy to design d^{10} metal-based selective hydrogenation catalysts. The proposed mechanism for the Ag/Al_2O_3-catalyzed hydrogenation of a nitroaromatic compound is shown in Fig. 4.

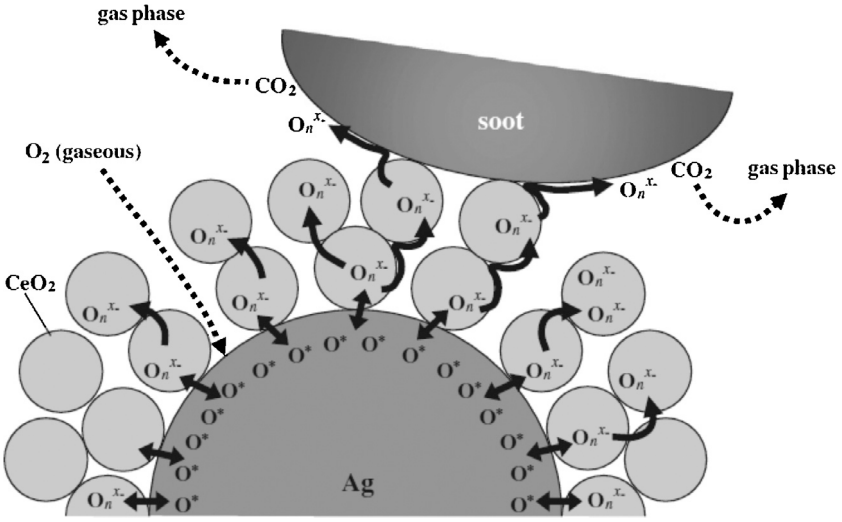

Fig. 3. Schematic mechanism for soot oxidation over the CeO_2-Ag catalyst [64].

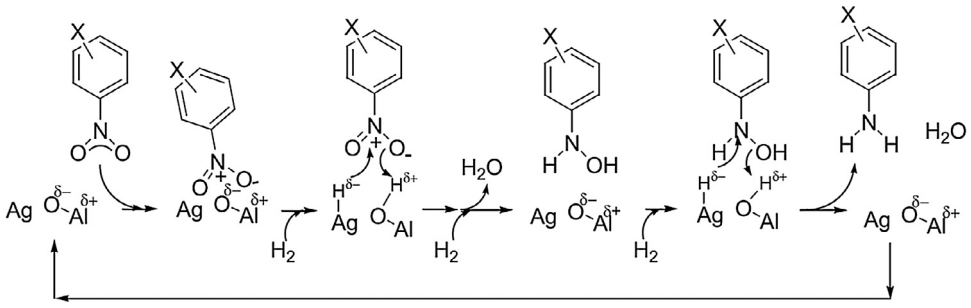

Fig. 4. Proposed mechanism for the Ag/Al_2O_3-catalyzed hydrogenation of nitroaromatic compounds [66].

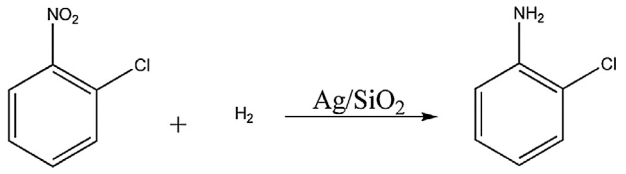

Fig. 5. Selective hydrogenation of *o*-chloronitrobenzene over Ag/SiO_2 catalyst to *o*-chloroaniline [6].

Saha et al. [68] reported an eco-friendly and cost effective heterogeneous biopolymer-supported Ag catalyst via a green photochemical synthetic approach. The calcium alginate-stabilized Ag catalyst exhibited even better catalytic performance than Au catalyst for the reduction of 4-nitrophenol to 4-aminophenol in the presence of excess borohydride as reducing agent. Chen et al. [6] developed a highly effective and recyclable Ag/SiO_2 catalyst via an in situ reduction method for the selective hydrogenation of a range of chloro-nitrobenzenes to their corresponding chloroanilines (see Fig. 5). The excellent catalytic performance of the Ag/SiO_2 catalyst could be attributed to the proper size of the silver nanoparticles as well as the interaction between the silver nanoparticles and the silica support.

Metallic Ag plays an important role in bimetallic catalytic systems. Bimetallic systems based on palladium with addition of silver are widely used as selective hydrogenation catalysts [69,70]. Gonzalez et al. [71] investigated the surface structure of Pd-Ag alloy and its alteration in the presence of atomic hydrogen using density functional (DFT) calculations on $Pd_{1-x}Ag_x$ (1 1 1) ($x = 0.2$). In the absence of an adsorbate, silver atoms segregate on the surface. At equilibrium, the surface is predicted to expose mainly Ag atoms. Isolated Pd atoms incorporated in this Ag-rich layer appear to be slightly preferred over the Pd_2 dimers. Increasing the coverage of adsorbed H atoms on the Pd-Ag substrate gradually suppresses surface segregation of silver, such that migration of all surface Ag atoms into the subsurface region becomes favorable at H coverage of ~0.25 ML. These results might have strong implications in understanding the role of Ag in promoting selective hydrogenation reactions over Pd-Ag catalysts. This notion of adsorbate-induced re-segregation in bimetallic systems is a general concept applicable to a broad variety of catalytic systems and advanced materials.

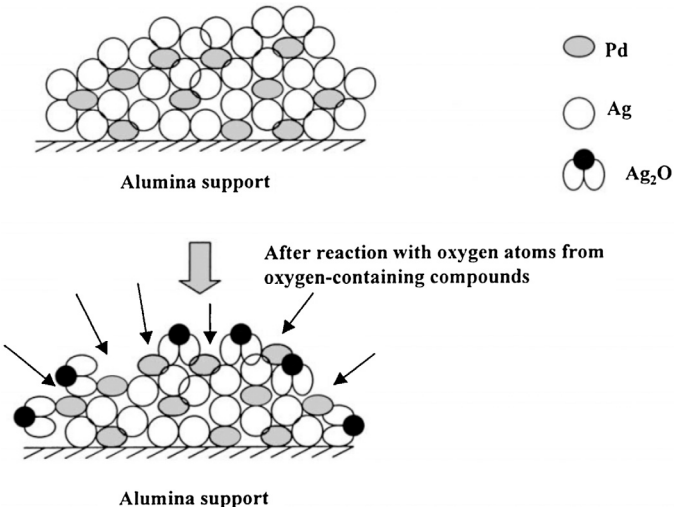

Fig. 7. Proposed model illustrating the effect of pre-treatment with oxygen and/or oxygen-containing compounds on enhancing the accessibility of Pd active sites responsible for the acetylene hydrogenation to ethylene [73].

He et al. [72] reported a novel Ag-Pd bimetallic catalyst supported on an ultrathin TiO_2 gel film prepared by a stepwise ion-exchange/reduction approach (see Fig. 6) and applied to the hydrogenation of methyl acrylate. The catalytic activity of the Pd-on-Ag nanoparticle is 367 times than that of commercial Pd black and 1.6 times as high as the Pd monometallic nanoparticles. The outstanding catalytic activity was attributed to the large fraction of the surface-exposed Pd atoms.

Praserthdam et al. [73] studied the catalytic performance of $Pd-Ag/Al_2O_3$ pretreated with O_2, NO_x and CO_x for the selective hydrogenation of acetylene in the presence of excess ethylene. The pretreatment with oxygen and/or oxygen-containing compounds resulted in the formation of Ag_2O, which is then exposed to the accessible Pd sites to react with C_2H_2 and H_2 in the feed stream. This enhances the catalytic activity of $Pd-Ag/Al_2O_3$ catalysts (See Fig. 7). The NO_x-treated catalysts gave higher ethylene yields because the number of sites for direct ethane formation was decreased in sharp contrast to O_2- or CO_x-treated catalysts.

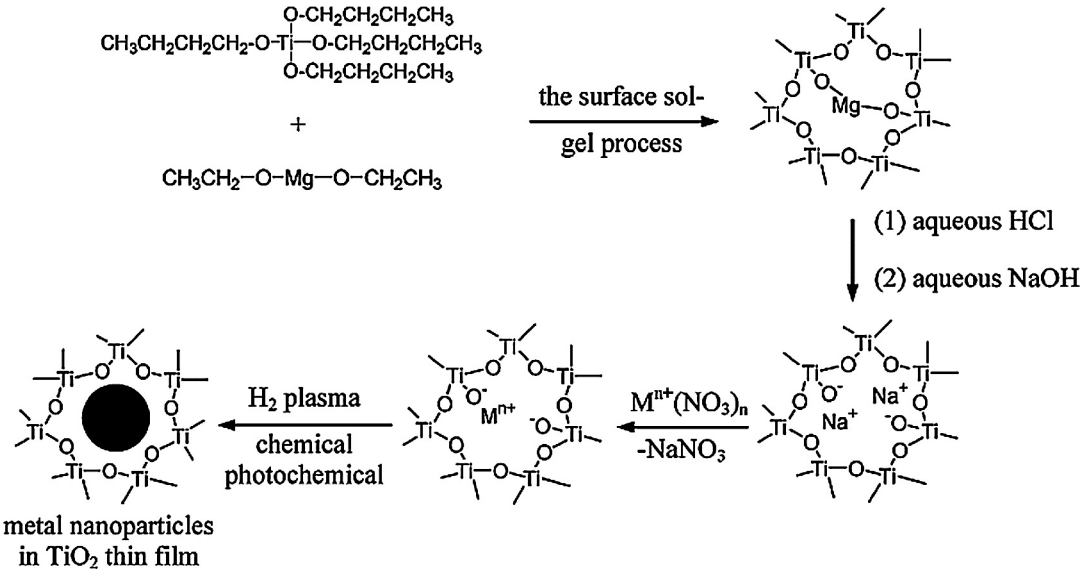

Fig. 6. Template approach to the incorporation of a noble metal ion into TiO_2 ultrathin films and subsequent nanoparticle formation [72].

Zhang et al. [74] reported a $PdAg/Al_2O_3$ alloy catalyst for the selective hydrogenation of acetylene. The activity of Pd-Ag catalyst is lower than that of pure Pd metal catalyst, however, the selectivity of Pd-Ag catalyst is higher and less impaired by temperature increases than traditional Pd catalyst. The addition of Ag to Pd catalyst decreases the quantity of adsorbed hydrogen and reduces adsorbed hydrogen spillover from the bulk of the metals to react with acetylene. This in turn increases the selectivity of acetylene hydrogenation to ethylene.

Mei et al. constructed a first principles-based kinetic Monte Carlo simulation and used it to follow the molecular transformations and kinetics in the selective hydrogenation of acetylene from ethylene feedstocks over the Pd-Ag alloy surfaces. [75] The kinetics for the hydrogenation of acetylene was established from the first-principles DFT calculations over the Pd-Ag alloy surfaces. The simulations reveal that the activity and the selectivity for acetylene hydrogenation are controlled by an optimal balance of hydrogen and ethylene on the surface. Alloying the surface with Ag results in both the ensemble and electronic effects that weaken the binding energies of acetylene and hydrogen to the surface. The presence of Ag on the surface also weakens the binding strengths for all surface intermediates including acetylene, vinyl, hydrogen and ethylene to increase their rates of desorption as well as their rates of hydrogenation. The presence of Ag on the Pd (1 1 1) surface also shuts down the larger Pd ensembles that can lead to C—C bond breaking as well as ethylidene formation.

Khan et al. [76,77] investigated the adsorption and co-adsorption of ethylene, acetylene and hydrogen on Pd-Ag particles supported on thin alumina films as a model catalyst by temperature programmed desorption (TPD). The TPD results show that the addition of Ag to Pd suppresses the overall hydrogenation activity but increases selectivity toward ethylene. Zea et al. [70] investigated how reconstruction of bimetallic Pd-Ag surfaces, and the presence of a co-adsorbed CO, work together to alter the reaction behavior of an industrially significant selective hydrogenation reaction.

Sales et al. [78] reported a $Pd-Ag/\gamma-Al_2O_3$ catalyst prepared by precipitation in a liquid polyol and applied it to the hydrogenation of hexa-1,5-diene in liquid phase at 40 °C. The addition of silver improved the hex-1-ene fractional selectivity in all cases, but lowered the catalyst activity when the Pd/Ag ratio was approximately unity. The Pd-rich bimetallic catalyst had very good activity and selectivity to hex-1-ene as well. The effects of silver addition are ascribed to the dilution of Pd atoms by silver atoms, which prevents the isomerization of hexa-1,5-diene.

2.3. Photocatalysis

2.3.1. Ag-based multiple-metal oxide photocatalysis

Multiple-metal oxides have been fabricated for the degradation of organic compounds or water splitting. Of the variety of multiple-metal oxide photocatalysts reported, special attention has been paid to materials containing metal ions with specific nd^{10} or $(nd^{10})\ ns^2$ outer layer orbital configurations including $AgInW_2O_8$, $AgNbO_3$, $AgGaO_2$ and Ag_2ZnGeO_4. A common feature of these catalysts is the completely filled nd^{10} or $(nd^{10})\ ns^2$ outer layer-orbitals that can hybridize with the O $2p^6$ orbitals in the valence band of a semiconducting material to increase the valence band top and thus lead to a narrowed band gap.

The Ag_2ZnGeO_4 [79] is an indirect semiconductor with a layered structure by a corner-connected tetrahedral (see Fig. 8). The band gap is 2.29 eV, which is much narrower than the gap (4.89 eV) of the isostructured Na_2ZnGeO_4 parent sample. The DFT calculation revealed that the Ag $4d^{10}$ orbitals have a profound impact on the band structure of Ag_2ZnGeO_4. The hybridized Ag $4d^{10}$ and O $2p^6$ orbitals form the valence band top of Ag_2ZnGeO_4 and contribute significantly to the narrowed band gap. The specific cristobalite structure of Ag_2ZnGeO_4 might be favorable for the separation and transportation of the photo-generated carriers. The unique energy band structure and crystal structure determined the overall photocatalytic performance of Ag_2ZnGeO_4.

2.3.2. Supported Ag photo-catalyst

Semiconductor photocatalysis is widely studied as the technological basis for solar energy storage cells, catalytic synthesis of organic compounds, and the degradation of organic contaminants in both the gas phase and aqueous systems. In addition, the green chemistry concept is generating excitement for efficient and stable photocatalysts in the visible light region. Semiconductor-based heterostructures with desired compositions and/or morphologies can modulate the properties of materials and find potential applications in photocatalysis. Currently, metal/semiconductor blends are one of the most popular heterostructures and have been extensively studied because of their excellent catalytic activity.

Ag/semiconductor is well studied because silver can trap the photogenerated electrons from the semiconductor and allow the holes to form hydroxyl radicals to degrade any organic species present. Moreover, silver can enhance the photocatalytic activity by creating a local electric field. The optical vibration of the surface plasmon in silver generates a reasonable enhancement in this electric field. When a noble metallic nanoparticle is excited by light, the oscillating electric field of the light interacts with the conduction

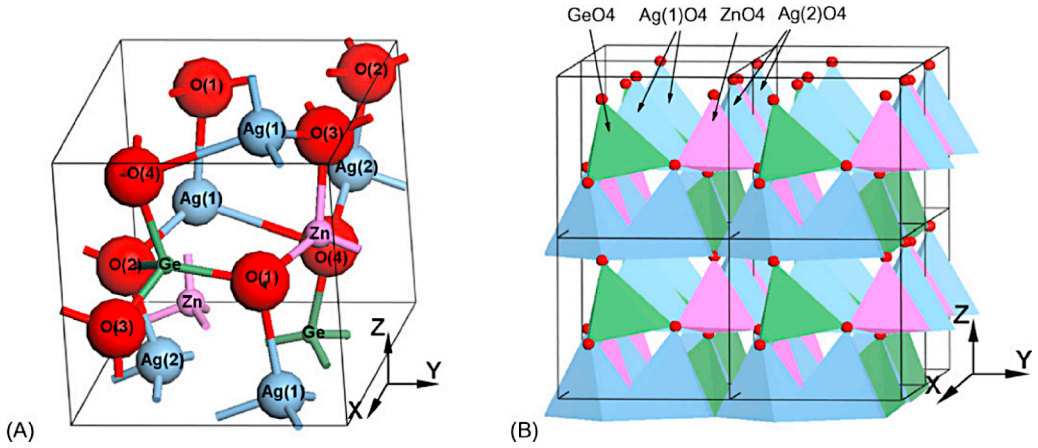

Fig. 8. The ball-and-stick model (A) and the polyhedron model (B) of Ag_2ZnGeO_4 [79].

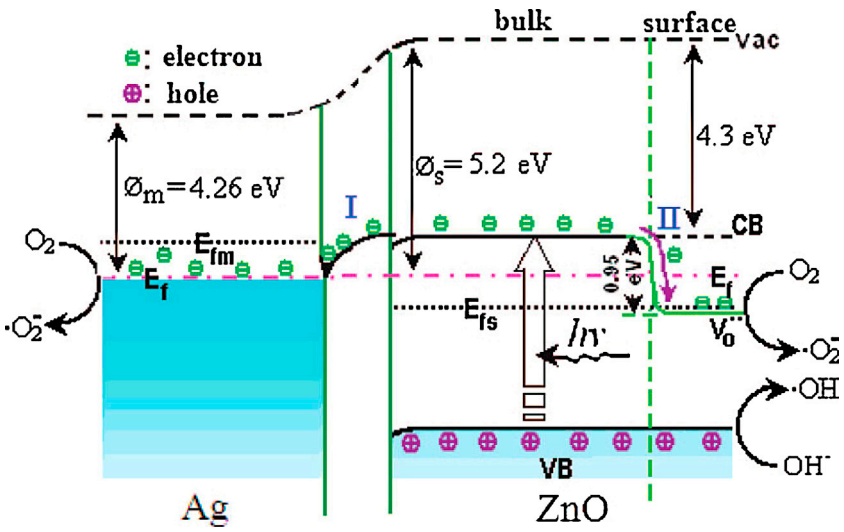

Fig. 9. Photo-generated electron transfer in Ag/ZnO nanocatalysts during the catalytic process. [a]ø: work function; E_f: Fermi level; $V_0^{\bullet\bullet}$: oxygen vacancy; CB: conduction band; VB: valence band; vac: vacuum level; m: metal; and s: semiconductor [80].

electrons. As a result, a strong oscillation of these electrons happens when the incident photon frequency is resonant with the collective oscillation of the conduction electrons. Such a resonance is called localized SPR for metallic nanoparticles. By engineering the size, shape and dielectric environment of the metallic nanoparticles, their absorption and scattering properties can be flexibly tuned. The localized SPR of silver nanoparticles usually results in strong and broad absorption bands in the visible light region and has been exploited to develop visible light-activated photocatalysts.

The increased photocatalytic activity of silver-modified ZnO is reportedly due to the changes in the surface properties such as oxygen vacancies and crystal defects [80]. Using the photocatalytic performance of a semiconductor-based heterostructure photocatalyst as an example, it is mainly dependent on the concentration of the heterostructure interface and defects, which can increase the separation efficiency of the photogenerated electron-hole pairs. The Ag/ZnO heterostructure photocatalyst has high catalytic activity and has attracted much research attention. The Ag nanoparticles and oxygen vacancy defects on the surface of ZnO nanocrystals benefit from the separation of photogenerated electron-hole pairs. This enhances the photocatalytic activity. Furthermore, there are two different pathways to transfer the photogenerated electrons from ZnO semiconductor to the dye for Ag/ZnO photocatalyst (see Fig. 9) upon irradiation by UV light [80].

Ag/TiO_2 is another popular photocatalyst that has already been studied by several research groups. Xin et al. [81] developed a new Ag/TiO_2 catalyst using a modified sol-gel method in the dark. AgO and Ag_2O are the main chemical states, and Ag ions inside the crystal lattice and the surface deposited Ag coexist. The appropriate amount of Ag offers abundant electronic traps and favors the transfer of the electrons to surface Ag. As a result, the recombination of photoinduced charge carriers can effectively be inhibited. Furthermore, Wen et al. [82] utilized both the SPR effect of Ag nanoparticles and the excellent electrical properties of graphene to design a new visible light-activated Ag/anatase-TiO_2/graphene. This product exhibited enhanced photo-catalytic activity in the degradation of methylene blue under visible light irradiation. In this photocatalyst, the loading of Ag nanoparticles enhances its optical response to a wider wavelength. The introduction of graphene not only accelerates the separation of photogenerated electron-hole pairs, but also enhances the adsorption capacity of the photocatalyst thereby improving the photocatalytic activity of TiO_2 under visible light irradiation. The coupling of graphene to improve the photocatalytic activity of TiO_2 could be applied to other wide bandgap semiconductors, while the introduction of noble metallic nanoparticles can further boost the photocatalytic efficiency. Because the SPR effect of noble metallic nanoparticles strongly depends on their species, size and shape, the optical response of nanocomposites

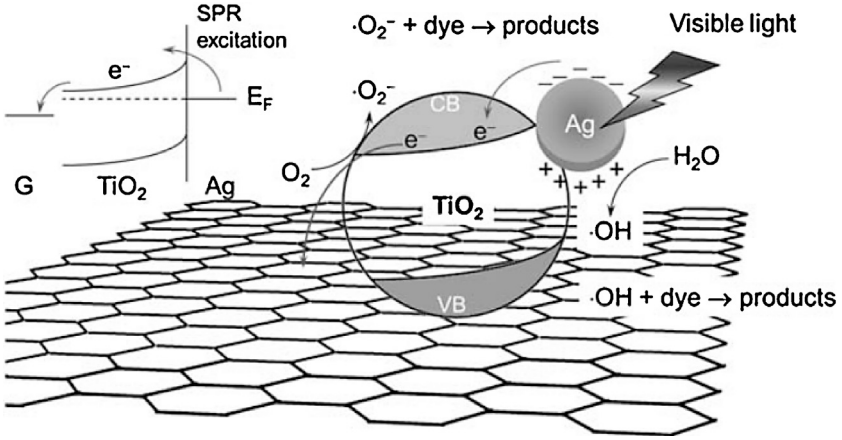

Fig. 10. Proposed mechanism for the photocatalytic degradation of organic dyes over Ag/TiO_2/G nanocomposites under visible light irradiation [82].

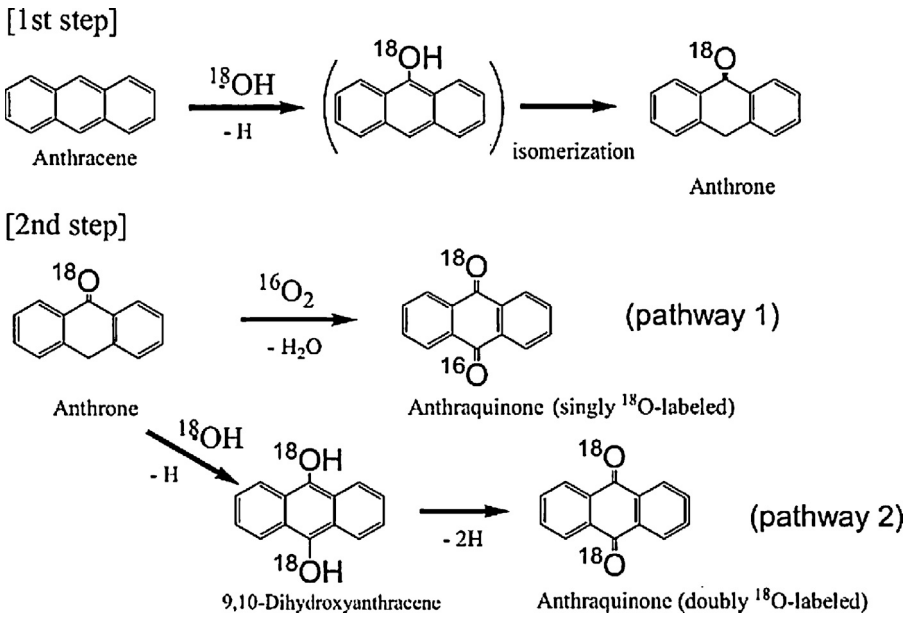

Fig. 11. Photocatalytic oxidation mechanism of anthracene on $AgBiVO_4$ [83].

of graphene and wide bandgap semiconductors can be flexibly tuned to further extend their absorption of sunlight and enhance their photocatalytic activity. The proposed mechanism is shown in Fig. 10.

Recently, $BiVO_4$ materials with a narrower band gap (2.4 eV) showed good photocatalytic performance. Kohtani et al. [83] developed a $Ag/BiVO_4$ photocatalyst for the photooxidation of polycyclic aromatic hydrocarbons (see Fig. 11). Compared to pure $BiVO_4$, this photocatalyst remarkably improves adsorptive and photooxidative performance via the degradation of long-chain alkylphenols. This is attributed to the synergetic effects on the specific adsorption property and efficient electron-hole separation at the $Ag/BiVO_4$ interface.

Cocatalyst modification is another efficient strategy to improve the photocatalytic efficiency of photocatalysts by promoting the effective separation of photogenerated electrons and holes. Yu et al. [84] found that the Ag_2O cocatalyst coated on the surface of Bi_2WO_6 nanoparticles via impregnation followed by low-temperature treatment (100–350 °C) offered much higher photocatalytic activity than the unmodified Bi_2WO_6 nanoparticles and N-doped TiO_2 for the decolorization of methyl orange solution under visible-light irradiation. The $Ag\text{-}Ag_2O$ composite easily formed during the decomposition of organics because of the photosensitive property of pure Ag_2O phase. The $Ag\text{-}Ag_2O$ can also act as a new and effective cocatalyst for the enhanced photocatalytic performance of photocatalysts (see Fig. 12) to provide a new approach for the design and development of high-performance visible-light photocatalysts.

The synergetic effect of the noble metal and semiconductor is important for improvement of the performance of nanocomposites in photocatalytic applications. In addition, Cao et al. developed a phase-controlled Ag/Sb_2S_3 photocatalyst [85] with silver nanoparticles dispersed on the surface of the hollow Sb_2S_3 sphere, which exhibited a high photocatalytic activity for the rapid degradation of 2-chlorophenol (see Fig. 13).

2.3.3. Ag/AgX photocatalyst

Silver halides (AgCl, AgBr and AgI) have been reported to be a new visible light photocatalytic material with good sensitivity to light. In the photocatalysis process, the silver halides absorb a photon and generate an electron and a positive hole. The photogenerated electron combines with Ag^+ to form Ag atoms. During

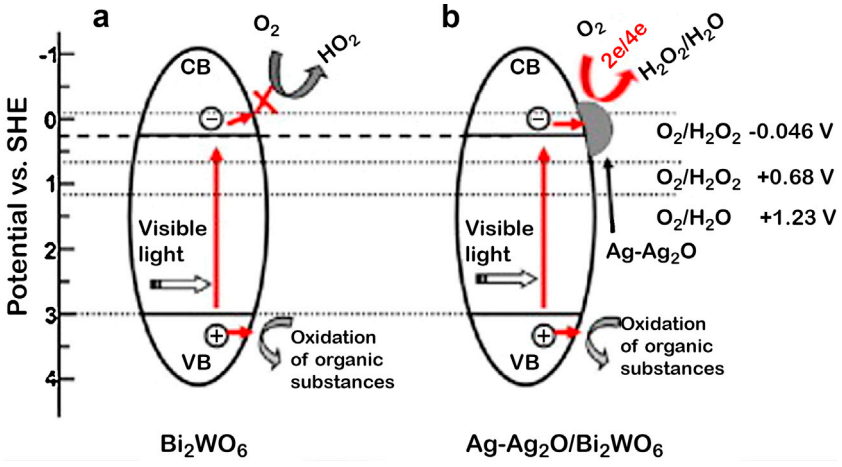

Fig. 12. Photocatalytic pathway on Ag/Bi_2WO_6 [84].

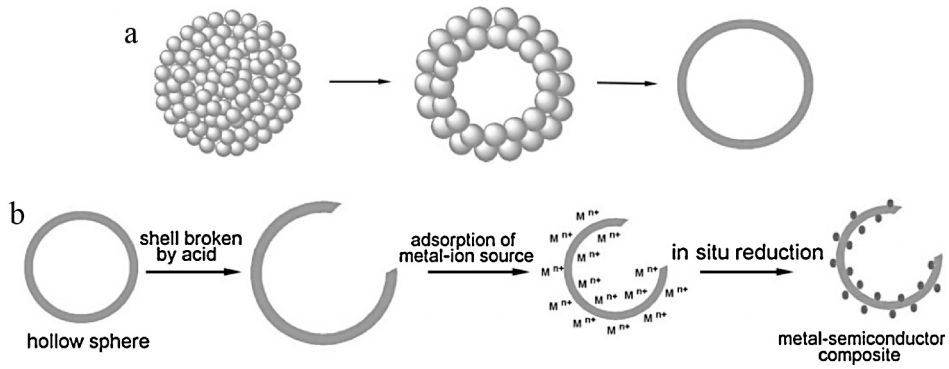

Fig. 13. Proposed synthetic approach for Ag/hollow Sb_2S_3 sphere. (a) Formation of hollow spheres via Ostwald ripening. (b) Formation of the composite structure of noble-metal nanoparticles and hollow spheres by the in situ reduction of adsorbed ions [85].

photocatalysis, the silver halide is usually loaded on some other materials to functionate its catalytic property. Thus, the catalytic property of silver halides rarely plays a main role in these catalysts, resulting in poor efficiency. Considering the SPR effect of noble metal nanoparticles, some highly efficient visible light plasmonic photocatalysts have been further fabricated. For example, Zang et al. [86] prepared a photocatalyst AgBr/Y-zeolite, which is highly efficient under sunlight. Some other visible light photocatalysts such as Ag@AgCl and Ag@AgBr have been developed recently [87–91]. Kuai et al. [92] reported a stable and highly efficient direct sunlight plasmonic Ag-AgBr photocatalyst through a facile hydrothermal and subsequent sunlight-induced route. The product removed more than 83% of pollutants and MO dye within 2 min of sunlight irradiation. The preparation of Ag@AgBr and proposed plasmonic photocatalytic mechanism is shown in Fig. 14. Elahifard et al. [93] demonstrated that Ag/AgBr/TiO_2-covered apatite has a high ability to adsorb bacteria in the dark and also has a significantly high photocatalytic activity under visible light for the destruction of bacteria.

3. Electrocatalysis

Ag-based catalysts have also been widely used in the electrocatalytic oxidation. Silver is a promising replacement for platinum because it has similar mechanisms and kinetics for catalytic oxygen reduction reactions (ORR). Ag has a higher tolerance toward methanol poisoning than Pt and rapidly decomposes hydroxide ions that can form peroxides known to cause membrane degradation. While no single metal can catalyze the ORR as effectively as Pt, it has been suggested that the high Ag overpotential could be reduced by alloying Ag with other selected metals.

The morphology of the catalysts is another important factor in the silver-based bi-metallic electrocatalysts because of the enhanced catalytic activity produced through electronic modification of the bimetallic structure. This enhancement is caused by the ligand effect that changes the d-band position and affects the adsorption, activation energies and charge transfer. Sekol et al. [94] studied silver palladium core-shell catalysts supported on multiwalled carbon nanotubes (Ag@Pd/MWNTs) (see Fig. 15) that are highly active and alcohol tolerant for the ORR reaction in alkaline media. In the presence of methanol, the Ag@Pd/MWNTs decreased the current density by 0.18 mA/cm^2 versus Pt/C (0.97 mA/cm^2) and Pd/C (1.09 mA/cm^2). In the presence of ethanol, the Ag@Pd/MWNTs' current density decreased by 0.12 mA/cm^2 versus Pt/C (0.87 mA/cm^2) and Pd/C (2.13 mA/cm^2). The Ag@Pd/MWNTs also show improved durability with an increased mass activity ~3.5 times higher than that of standard Pd/C after durability testing in ethanol.

The methanol oxidation reaction (MOR) at the anode of direct methanol fuel cells (DMFCs) plays a key role in controlling the performance of a fuel cell, and efficient MOR electrocatalysts are essential for practical applications of fuel cells. Protons are produced when methanol gas flow permeates the anode catalyst layer. This increases the distance of the methanol gas across the anode, and the catalyst layer enhances the MOR and fuel cell performance. For this purpose, it is critical to not only increase the specific surface area of the catalysts with good electrical conductivity, but also to reduce the cost and develop a facile synthesis route.

Tang et al. [95] synthesized a flexible and uniquely network-structured polyaniline (PANi) and polypyrrole (PPy) supported Ag catalysts for MOR in PEMFC applications. Wang et al. [96] developed a hybrid nanomaterial catalyst consisting of graphene nanosheets supporting Ag nanoparticles via a one-pot reduction method and applied it to the electrochemical oxidation of methanol in alkaline solution (see Fig. 16). The enhanced catalytic performance could

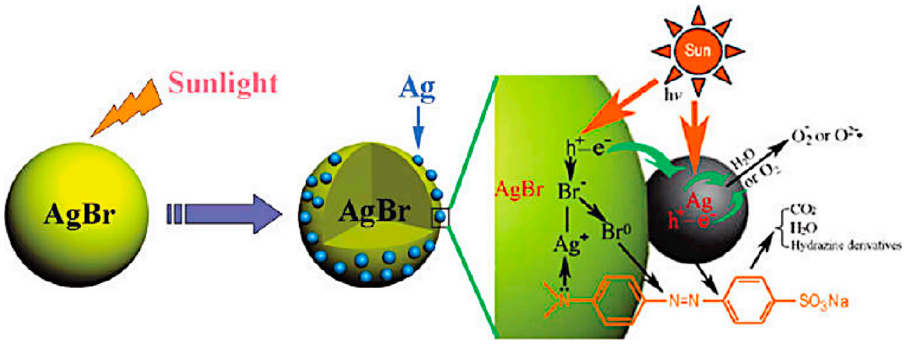

Fig. 14. The proposed photocatalytic mechanism of a Ag-AgBr plasmonic photocatalyst [92].

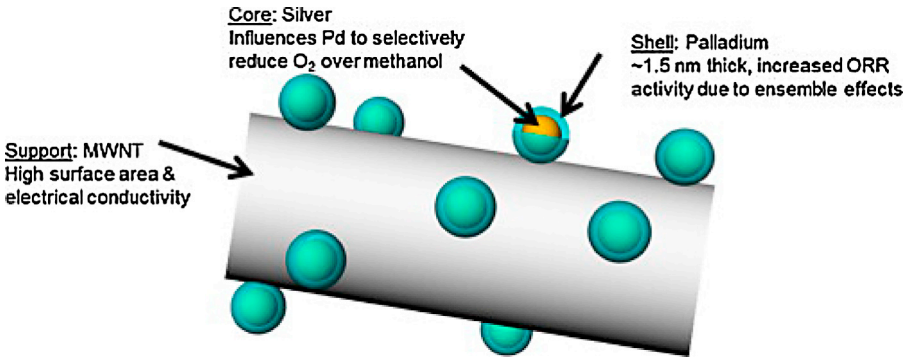

Fig. 15. The simulation mechanism of the Ag@Pd/MWNTs catalyst for the ORR reaction [94].

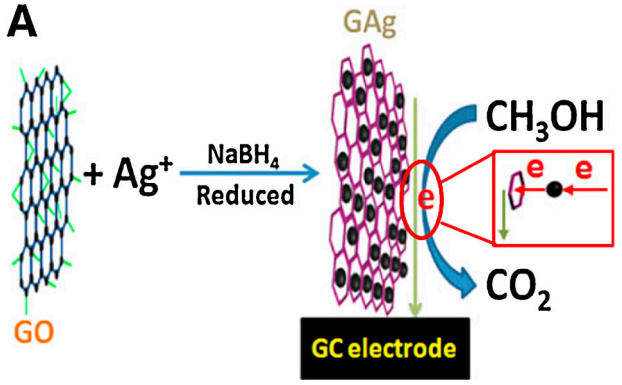

Fig. 16. Scheme of preparation and electrochemical catalytic reaction of GAg [96].

be attributed to the high conductivity of graphene and the high dispersion of Ag nanoparticles.

According to the *d*-band theory of Nørskov and co-workers, reactivity will increase as a function of d-band center values for the overlayer and impurity atoms. The d-band center shifts up in metals with small lattice constants and vice versa. This subsequently affects the reaction rate [97]. If the d-band center increases, the adsorption affinity of the adsorbate for the metals will be stronger and this may help to improve the electrooxidation of ethanol on the surface of the metals. Nguyen et al. [98] reported the synthesis of an alloyed Pd-Ag/C catalyst by a co-reduction method, which exhibited great synergetic effects for the ethanol electrooxidation.

Generally, the metal interaction caused by the introduction of a second metal component would be helpful for the silver-based electrocatalyst due to the synergistic effects generated at the interface of the metals, specific morphologies, or the ligand effect. Miller et al. [99] investigated a series of nanostructured electrocatalysts AgPd/C(600), FePd/C(600) and FeAgPd/C(600) (ca. 3 wt% metal loadings) for the ORR reaction in alkaline media and found that both of the Fe-containing electrocatalysts—FeAgPd/C(600) and FePd/C(600)—were highly active for the ORR. They exclusively promoted the four electron pathway during chronopotentiometry, while AgPd/C(600) produced up to 35 mol% HO_2^-. Compared to FePd/C(600), the binary FeAgPd/C(600) catalyst had a remarkably higher activity and stability. The experimental evidence could be explained in terms of a synergistic Ag-Fe interaction that results

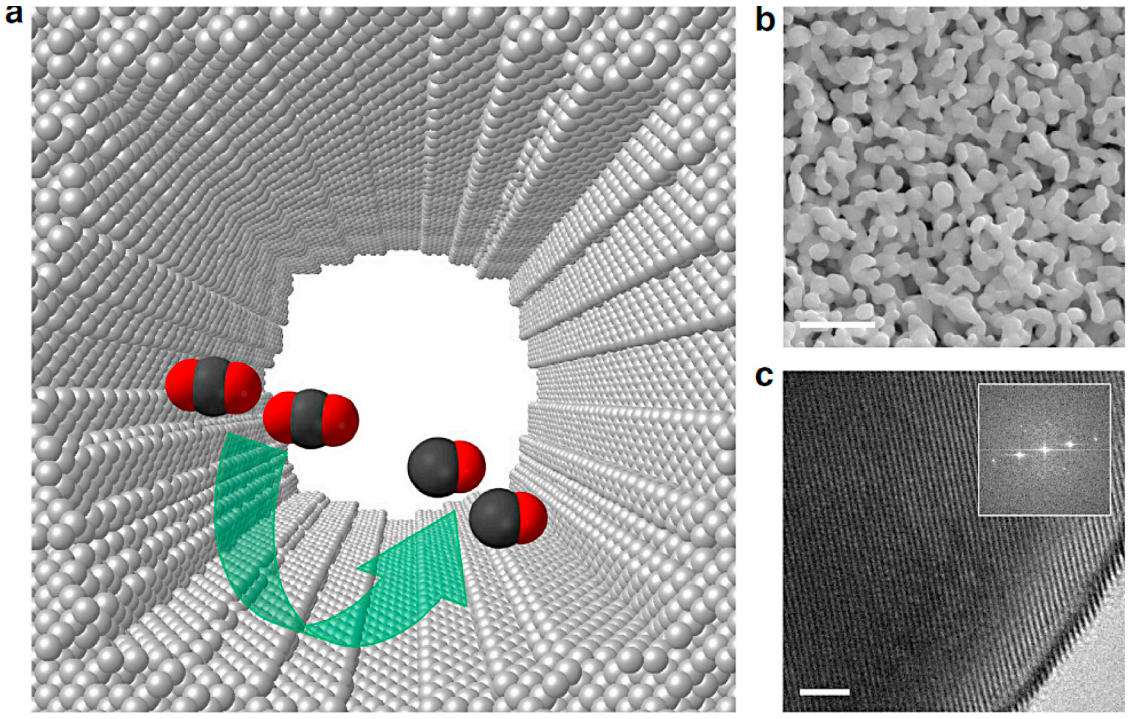

Fig. 17. (a) Diagram of a silver electrocatalyst nanopore with highly curved internal surface. (b) SEM of NP-Ag (c) TEM of NP-Ag [100].

from the unique nanostructure that forms during heat treatment and consists of very finely dispersed Ag nanoparticles.

Silver is also an interesting electrocatalyst because of its ability to convert carbon dioxide to carbon monoxide selectively at room temperature. The Ag-based catalysts could also convert carbon dioxide to useful chemicals selectively and efficiently. Lu et al. [100] developed a nanoporous silver electrocatalyst (see Fig. 17) that electrochemically reduces carbon dioxide to carbon monoxide with approximate 92% selectivity at a rate that is currently over 3000 times higher than the traditional polycrystalline counterpart under moderate overpotentials of lower than 0.50 V because of the large electrochemical surface area of the NP-Ag catalyst. The as-synthesized NP-Ag catalysts could stabilize the CO_2^- intermediates on the highly curved surface, resulting in the smaller overpotentials needed to overcome these thermodynamic barriers.

4. Outlook

The development of nano-synthetic technology including novel silver-based heterogeneous nanocatalysts will be increasingly applied in more and more green chemistry processes due to their selective hydrogenation and oxidation reactions. Until recently, only two commercial silver-based catalysts are available including electrolytic silver and Ag/Al_2O_3, which were used in the production of formaldehyde from the oxidation of methanol and the epoxidation of ethylene to ethylene oxide. Nonetheless, research continues in both academic and commercial organizations to develop novel silver based catalysts with highly catalytic performance in large quantity and high stability. The catalytic procedure in a more moderate and less pollutional condition can be still a longstanding goal for the catalytic oxidation and reduction process by using Ag based catalysts; meanwhile, controllable synthesis of highly stable and distributed Ag nanoparticles with small size and narrow size-distribution is still a great challenge. Furthermore, in the burgeoning photocatalytic process, Ag based heterogeneous catalysts would also play significant roles because of the superb capacity of the response to visible light. More and more Ag nanocomponents with high separation ability of photogenerated charges and high degradation efficiency will translate laboratory-scale academic research into scalable, manufacturable technologies to meet the demands of the efficient utilization of solar energy. Moreover, Ag based electrocatalyst exhibits reasonable activity and stability with the price only about 1% that of Pt, rendering it as an attractive ORR catalyst. Ag based catalysts are more adaptive to be used in alkaline electrolytes and are promising cathode materials with good balance between cost and performance. More importantly, Ag-based elecrtocatalysts exhibit considerable ORR reactivity even within highly concentrated alkaline media and at elevated temperature, making them more profound of academic and practical significance including the fast-growing metal-air battery applications. It is reasonable to believe that new catalysts and/or catalytic processes based on silver-containing materials will continue to be explored in the near future.

Acknowledgements

We would like to thank financial support by the Major State Basic Research Development Program (Grant No. 2012CB224804), NSFC (Project 21373054, 21173052), the Natural Science Foundation of Shanghai Science and Technology Committee (08DZ2270500). We also thank LetPub (www.letpub.com) for its linguistic assistance during the preparation of this manuscript.

References

[1] X.E. Verykios, F.P. Stein, R.W. Coughlin, Catal. Rev. Sci. Eng. 22 (1980) 197–234.
[2] W. Grünert, A. Brückner, H. Hofmeister, P. Claus, J. Phys. Chem. B 108 (2004) 5709–5717.
[3] P. Claus, H. Hofmeister, J. Phys. Chem. B 103 (1999) 2766–2775.
[4] M. Bron, D. Teschner, A. Knop-Gericke, F.C. Jentoft, J. Kröhnert, J. Hohmeyer, C. Volckmar, B. Steinhauer, R. Schlögl, P. Claus, Phys. Chem. Chem. Phys. 9 (2007) 3559–3569.
[5] M. Steffan, A. Jakob, P. Claus, H. Lang, Catal. Commun. 10 (2009) 437–441.
[6] Y. Chen, C. Wang, H. Liu, J. Qiu, X. Bao, Chem. Commun. (2005) 5298–5300.
[7] H. Zhang, Q. Fu, Y. Yao, Z. Zhang, T. Ma, D. Tan, X. Bao, Langmuir 24 (2008) 10874–10878.
[8] M. Kreich, P. Claus, Angew. Chem. Int. Ed. 44 (2005) 7800–7804.
[9] K. Shimizu, K. Ohshima, A. Satsuma, Chem. Eur. J 15 (2009) 9977–9980.
[10] T. Mitsudome, S. Arita, H. Mori, T. Mizugaki, K. Jitsukawa, K. Kaneda, Angew. Chem. 120 (2008) 8056–8058.
[11] T. Mitsudome, A. Noujima, Y. Mikami, T. Mizugaki, K. Jitsukawa, K. Kaneda, Angew. Chem. 122 (2010) 5677–5680.
[12] M.J. Beier, T.W. Hansen, J.-D. Grunwaldt, J. Catal. 266 (2009) 320–330.
[13] B. Hammer, J. Nørskov, Surf. Sci. 343 (1995) 211–220.
[14] A.B. Mohammad, I.V. Yudanov, K.H. Lim, K.M. Neyman, N. Rösch, J. Phys. Chem. C 112 (2008) 1628–1635.
[15] A. Montoya, A. Schlunke, B.S. Haynes, J. Phys. Chem. B 110 (2006) 17145–17154.
[16] X. Bao, M. Muhler, T. Schedel-Niedrig, R. Schlögl, Phys. Rev. B 54 (1996) 2249.
[17] A. Michaelides, K. Reuter, M. Scheffler, J. Vac. Sci. Technol. A 23 (2005) 1487–1497.
[18] R. Van Santen, H. Kuipers, Adv. Catal. 35 (1987) 265–321.
[19] W.L. Dai, Y. Cao, L.P. Ren, X.L. Yang, J.H. Xu, H.X. Li, H.Y. He, K.N. Fan, J. Catal. 228 (2004) 80–91.
[20] J.H. Lee, S.J. Schmieg, S.H. Oh, Appl. Catal. A: Gen. 342 (2008) 78–86.
[21] L. Zhang, C.B. Zhang, H. He, J. Catal. 261 (2009) 101.
[22] R. Yamamoto, Y. Sawayama, H. Shibahara, Y. Ichihashi, S. Nishiyama, S. Tsuruya, J. Catal. 234 (2005) 308–317.
[23] A.J. Nagy, G. Mestl, R. Schlögl, J. Catal. 188 (1999) 58–68.
[24] V. Purcar, D. Donescu, C. Petcu, R. Luque, D.J. Macquarrie, Appl. Catal. A: Gen. 363 (2009) 122–128.
[25] O. Magaev, A. Knyazev, O. Vodyankina, N. Dorofeeva, A. Salanov, A. Boronin, Appl. Catal. A: Gen. 344 (2008) 142–149.
[26] R. Xu, X. Wang, D. Wang, K. Zhou, Y. Li, J. Catal. 237 (2006) 426–430.
[27] A.Q. Wang, J.H. Liu, S. Lin, T.S. Lin, C.-Y. Mou, J. Catal. 233 (2005) 186–197.
[28] A. Wang, Y.-P. Hsieh, Y.-F. Chen, C.-Y. Mou, J. Catal. 237 (2006) 197–206.
[29] X. Wei, X.F. Yang, A.-Q. Wang, L. Li, X.Y. Liu, T. Zhang, C.Y. Mou, J. Li, J. Phys. Chem. C 116 (2012) 6222–6232.
[30] H. Liu, D. Ma, R.A. Blackley, W. Zhou, X. Bao, Chem. Commun. (2008) 2677–2679.
[31] X. Bao, M. Muhler, B. Pettinger, R. Schlögl, G. Ertl, Catal. Lett. 22 (1993) 215–225.
[32] X. Bao, M. Muhler, R. Schlögl, G. Ertl, Catal. Lett. 32 (1995) 185–194.
[33] H. Schubert, U. Tegtmeyer, D. Herein, X. Bao, M. Muhler, R. Schlögl, Catal. Lett. 33 (1995) 305–319.
[34] D.S. Su, T. Jacob, T.W. Hansen, D. Wang, R. Schlögl, B. Freitag, S. Kujawa, Angew. Chem. 120 (2008) 5083–5086.
[35] Z. Qu, M. Cheng, W. Huang, X. Bao, J. Catal. 229 (2005) 446–458.
[36] C.J. Bertole, C.A. Mims, J. Catal. 184 (1999) 224–235.
[37] X. Zhang, Z. Qu, X. Li, Q. Zhao, Y. Wang, X. Quan, Catal. Commun. 16 (2011) 11–14.
[38] R.R. Hu, C.F. Yan, L.Y. Xie, Y. Cheng, D.Z. Wang, Int. J. Hydrogen Energy 36 (2011) 64–71.
[39] L.P. Ren, W.L. Dai, Y. Cao, K.N. Fan, Catal. Lett. 85 (2003) 81–85.
[40] L.P. Ren, W.L. Dai, Y. Cao, H.X. Li, W.H. Zhang, K.N. Fan, Acta Chim. Sinica 61 (2003) 937–940.
[41] L.P. Ren, W.L. Dai, X.L. Yang, Y. Cao, H. Li, K.N. Fan, Appl. Catal. A: Gen. 273 (2004) 83–88.
[42] L.P. Ren, W.L. Dai, Y. Cao, H. Li, K. Fan, Chem. Commun. (2003) 3030–3031.
[43] A. Ishige, Y., Murasawa, F. Honda, JP Pat. 49-24889 (1995).
[44] J.O. Punderson, US Pat. 2 939 83 (1960).
[45] R.S. Aries, US Pat. 2 953 602 (1960).
[46] S. Sago, JP Pat. 61-130252 (1986).
[47] M. Sago, JP Pat. 60-89441 (1985).
[48] C. Wang, H. Yin, S. Dai, S. Sun, Chem. Mater. 22 (2010) 3277–3282.
[49] Y. Iizuka, T. Miyamae, T. Miura, M. Okumura, M. Daté, M. Haruta, J. Catal. 262 (2009) 280–286.
[50] D.I. Kondarides, X.E. Verykios, J. Catal. 158 (1996) 363–377.
[51] A. Sandoval, A. Aguilar, C. Louis, A. Traverse, R. Zanella, J. Catal. 281 (2011) 40–49.
[52] J.H. Liu, A.Q. Wang, Y.S. Chi, H.P. Lin, C.-Y. Mou, J. Phys. Chem. B 109 (2005) 40–43.
[53] C.W. Yen, M.L. Lin, A. Wang, S.A. Chen, J.M. Chen, C.Y. Mou, J. Phys. Chem. C 113 (2009) 17831–17839.
[54] A. Wittstock, V. Zielasek, J. Biener, C. Friend, M. Bäumer, Science 327 (2010) 319–322.
[55] K.M. Kosuda, A. Wittstock, C.M. Friend, M. Bäumer, Angew. Chem. Int. Ed. 51 (2012) 1698–1701.
[56] L.V. Moskaleva, S. Röhe, A. Wittstock, V. Zielasek, T. Klüner, K.M. Neyman, M. Bäumer, Phys. Chem. Chem. Phys. 13 (2011) 4529–4539.
[57] L. Liotta, A. Venezia, G. Deganello, A. Longo, A. Martorana, Z. Schay, L. Guczi, Catal. Today 66 (2001) 271–276.

[58] N.K. Chaki, H. Tsunoyama, Y. Negishi, H. Sakurai, T. Tsukuda, J. Phys. Chem. C 111 (2007) 4885–4888.
[59] X. Huang, X. Wang, X. Wang, X. Wang, M. Tan, W. Ding, X. Lu, J. Catal. 301 (2013) 217–226.
[60] S. Hirasawa, H. Watanabe, T. Kizuka, Y. Nakagawa, K. Tomishige, J. Catal. 300 (2013) 205–216.
[61] E. Aneggi, J. Llorca, C. de Leitenburg, G. Dolcetti, A. Trovarelli, Appl. Catal. B: Environ. 91 (2009) 489–498.
[62] M. Machida, Y. Murata, K. Kishikawa, D. Zhang, K. Ikeue, Chem. Mater. 20 (2008) 4489–4494.
[63] K. Shimizu, H. Kawachi, A. Satsuma, Appl. Catal. B: Environ. 96 (2010) 169–175.
[64] K. Yamazaki, T. Kayama, F. Dong, H. Shinjoh, J. Catal. 282 (2011) 289–298.
[65] H.U. Blaser, H. Steiner, M. Studer, ChemCatChem 1 (2009) 210–221.
[66] K. Shimizu, Y. Miyamoto, A. Satsuma, J. Catal. 270 (2010) 86–94.
[67] K. Shimizu, Y. Miyamoto, T. Kawasaki, T. Tanji, Y. Tai, A. Satsuma, J. Phys. Chem. C 113 (2009) 17803–17810.
[68] S. Saha, A. Pal, S. Kundu, S. Basu, T. Pal, Langmuir 26 (2009) 2885–2893.
[69] P.A. Sheth, M. Neurock, C.M. Smith, J. Phys. Chem. B 109 (2005) 12449–12466.
[70] H. Zea, K. Lester, A.K. Datye, E. Rightor, R. Gulotty, W. Waterman, M. Smith, Appl. Catal. A: Gen. 282 (2005) 237–245.
[71] S. Gonzalez, K.M. Neyman, S. Shaikhutdinov, H.-J. Freund, F. Illas, J. Phys. Chem. C 111 (2007) 6852–6856.
[72] J. He, T. Kunitake, Chem. Mater. 16 (2004) 2656–2661.
[73] P. Praserthdam, B. Ngamsom, N. Bogdanchikova, S. Phatanasri, M. Pramotthana, Appl. Catal. A: Gen. 230 (2002) 41–51.
[74] Q. Zhang, J. Li, X. Liu, Q. Zhu, Appl. Catal. A: Gen. 197 (2000) 221–228.
[75] D. Mei, M. Neurock, C.M. Smith, J. Catal. 268 (2009) 181–195.
[76] N. Khan, S. Shaikhutdinov, H.-J. Freund, Catal. Lett. 108 (2006) 159–164.
[77] N. Khan, A. Uhl, S. Shaikhutdinov, H.-J. Freund, Surf. Sci. 600 (2006) 1849–1853.
[78] E. Andrade Sales, B. Benhamida, V. Caizergues, J.-P. Lagier, F. Fiévet, F. Bozon-Verduraz, Appl. Catal. A: Gen. 172 (1998) 273–283.
[79] X. Li, S. Ouyang, N. Kikugawa, J. Ye, Appl. Catal. A: Gen. 334 (2008) 51–58.
[80] F. Zhang, Y. Zheng, Y. Cao, C. Chen, Y. Zhan, X. Lin, Q. Zheng, K. Wei, J. Zhu, J. Mater. Chem. 19 (2009) 2771–2777.
[81] D. Lin, H. Wu, R. Zhang, W. Pan, Chem. Mater. 21 (2009) 3479–3484.
[82] Y. Wen, H. Ding, Y. Shan, Nanoscales 3 (2011) 4411–4417.
[83] S. Kohtani, M. Tomohiro, K. Tokumura, R. Nakagaki, Appl. Catal. B: Environ. 58 (2005) 265–272.
[84] L. Zhang, H. Wang, Z. Chen, P.K. Wong, J. Liu, Appl. Catal. B: Environ. 106 (2011) 1–13.
[85] X. Cao, L. Gu, L. Zhuge, W. Gao, W. Wang, S. Wu, Adv. Funct. Mater. 16 (2006) 896–902.
[86] Y. Zang, R. Farnood, J. Currie, Chem. Eng. Sci. 64 (2009) 2881–2886.
[87] P. Wang, B. Huang, X. Zhang, X. Qin, H. Jin, Y. Dai, Z. Wang, J. Wei, J. Zhan, S. Wang, Chem. Eur. J. 15 (2009) 1821–1824.
[88] Z. Zheng, B. Huang, X. Qin, X. Zhang, Y. Dai, M. Jiang, P. Wang, M.H. Whangbo, Chem. Eur. J. 15 (2009) 12576–12579.
[89] C. An, S. Peng, Y. Sun, Adv. Mater. 22 (2010) 2570–2574.
[90] P. Wang, B. Huang, Q. Zhang, X. Zhang, X. Qin, Y. Dai, J. Zhan, J. Yu, H. Liu, Z. Lou, Chem. Eur. J. 16 (2010) 10042–10047.
[91] Y. Bi, J. Ye, Chem. Eur. J. 16 (2010) 10327–10331.
[92] L. Kuai, B. Geng, X. Chen, Y. Zhao, Y. Luo, Langmuir 26 (2010) 18723–18727.
[93] M.R. Elahifard, S. Rahimnejad, S. Haghighi, M.R. Gholami, J. Am. Chem. Soc. 129 (2007) 9552–9553.
[94] R.C. Sekol, X. Li, P. Cohen, G. Doubek, M. Carmo1, A.D. Taylor, Appl. Catal. B: Environ. 138–139 (2013) 285–293.
[95] Q. Tang, J. Wu, Z. Tang, Y. Li, J. Lin, M. Huang, J. Mater. Chem. 21 (2011) 13354–13364.
[96] Y. Wang, S. Zhang, H. Chen, H. Li, P. Zhang, Z. Zhang, G. Liang, J. Kong, Electrochem. Commun. 17 (2012) 63–66.
[97] J. Greeley, J.K. Nørskov, Surf. Sci. 592 (2005) 104–111.
[98] S.T. Nguyen, H.M. Law, H.T. Nguyen, N. Kristian, S.Y. Wang, S.H. Chan, X. Wang, Appl. Catal. B: Environ. 113 (2012) 261–270.
[99] H.A. Miller, M. Bevilacqua, J. Filippi, A. Lavacchi, A. Marchionni, M. Marelli, S. Moneti, W. Oberhauser, E. Vesselli, M. Innocenti, F. Vizza, J. Mater. Chem. A 1 (2013) 13337–13347.
[100] Q. Lu, J. Rosen, Y. Zhou, G.S. Hutchings, Y.C. Kimmel, J.G. Chen, F. Jiao, Nat. Commun. 5 (2014) 3242.